Macromolecular diffusion in the extracellular matrix measured by fluorescence correlation spectroscopy

Nina Kristine Reitan
Aphirak Juthajan*
Tore Lindmo
Catharina de Lange Davies
The Norwegian University of Science and Technology
Department of Physics
7491 Trondheim, Norway

Abstract. Diffusion of therapeutic macromolecules through the extracellular matrix of tumor tissue is a crucial step in drug delivery. We use fluorescence correlation spectroscopy (FCS) to measure diffusion of IgG (150 kDa) and dextrans (155 kDa and 2 MDa) in solution, 5% gelatin hydrogel, and multicellular spheroids. Gel and spheroids are used as model systems for the extracellular matrix. The diffusion depends on the complexity of the environment, as well as on the size and structural shape of the diffusing molecules. The results based on one-photon FCS are in good agreement with diffusion coefficients obtained with two-photon fluorescence recovery after photobleaching (FRAP) using the same microscope (Zeiss LSM510 META/Confocor2). However, FCS reveals anomalous or multicomponent diffusion in gel and spheroids, which are not resolvable with FRAP. This study demonstrates that one-photon FCS can be used to study the extracellular transport of macromolecules in tumor tissue, and that FCS provides additional information about diffusion properties compared to FRAP.
 [DOI: 10.1117/1.2982530]

Keywords: fluorescence spectroscopy; correlation; tissues; confocal optics; diffusion; biology.

Paper 08046R received Feb. 5, 2008; revised manuscript received Jun. 9, 2008; accepted for publication Jun. 15, 2008; published online Oct. 14, 2008.

1 Introduction

The study of molecular dynamics in tissue provides valuable information about processes in the living organism. Insight into molecular binding, interactions, transport, and distribution, as well as the development of noninvasive techniques that provide such information, are crucial. In cancer research, it is important to acquire knowledge about delivery and pharmacokinetics of macromolecular anticancer agents (e.g., antibodies, liposomes, and DNA vectors), which are of great interest in therapy due to their specificity for tumor tissue. However, these large molecules have to overcome severe physiological barriers on their way from the blood vessels, through the extracellular matrix (ECM) and into the cancer cells, and only a minor fraction of the injected therapeutic macromolecules accumulates in tumor tissue.[1,2] Due to the high interstitial fluid pressure in tumors,[1,3] diffusion is the major interstitial transport mechanism. The ECM consists of a protein network embedded in a hydrophilic gel of glycosaminoglycans and proteoglycans, and this complex structure slows down diffusion of the therapeutic agents.[4] It is therefore of clinical importance to study diffusion and factors that influence transport behavior in the ECM.

Fluorescence correlation spectroscopy (FCS)[5,6] is a technique for measuring molecular dynamics and interactions, and the number of studies in living cells and tissue is increasing.[7–11] The principle of FCS is to detect intensity fluctuations from fluorescent molecules in a small detection volume defined by a focused laser beam. The temporal correlation of the intensity fluctuations yields valuable information about molecular properties like translational and rotational diffusion, interactions, concentration, and conformation changes. A low concentration of fluorescent molecules is essential to obtain proper correlation amplitudes, and this is an advantage when studying biological tissue.

FCS is a highly sensitive technique and not straightforward in complex systems like cellular environments. Heterogeneity, scattering, tissue absorption, low detection efficiency, photodamage, autofluorescence, and a distorted detection volume are all possible sources of error.[8,12] This degradation of information can partly be compensated for by increasing the laser power. This may, however, induce unwanted effects like autofluorescence, photobleaching, and optical saturation.[13,14]

Fluorescence recovery after photobleaching (FRAP) is an alternative technique for studying diffusion.[15] The basic principle is to photobleach fluorescent molecules in a chosen region of interest, and subsequently measure the rate of fluorescence recovery. As opposed to FCS, a high concentration of fluorophores is necessary to detect the influx of unbleached molecules during recovery. FRAP has a lower time resolution than FCS, because recovery may occur during the bleaching period in cases of fast diffusion. FRAP is therefore better suited for measuring slow diffusion on a time scale of milliseconds to seconds, whereas FCS operates best on a time scale of microseconds to milliseconds (the diffusion time window in the Confocor2 covers the range 0.2 μs to 1 s).[12] The

*Current affiliation: Carl Zeiss AS, 1086 Oslo, Norway.
Address all correspondence to: Nina Reitan, Dept. of Physics, Norwegian University of Science and Technology, Høgskoleringen 5, 7491 Trondheim, Norway; Tel: +47 73598709; Fax: +47 73597710; E-mail: nina.reitan@ntnu.no

1083-3668/2008/13(5)/054040/9/$25.00 © 2008 SPIE

highest diffusion coefficient that can be measured with two-photon FRAP is limited by the characteristic diffusion time and the bleaching time. According to Meyvis et al.,[16] the bleaching time should be less than 1/15 of the characteristic diffusion time, but a factor of 1/2 is also shown to be sufficient.[17]

Although FCS is a frequently used method for intracellular studies,[7–9,11,18] only a few FCS studies of extracellular diffusion in tissue have been published.[10] To our knowledge, there are no published results on extracellular diffusion in multicellular spheroids using FCS. In cellular environments, two-photon excitation has the advantage of increased depth penetration, reduced photobleaching, and a more well-defined detection volume.[8,19] However, the feasibility of one-photon FCS in living cells and tissue has been demonstrated.[8,20] The purpose of the present work was thus to explore the capabilities and limitations of a one-photon FCS system (ConfoCor2, Carl Zeiss Jena GmbH, Germany) to measure diffusion of macromolecules in tissue. Diffusion of IgG and dextran molecules was measured extracellularly in multicellular spheroids, as well as in gelatin hydrogel and solution, and compared to previously obtained results with FRAP.[17] Gel and spheroids were used as model systems for the ECM. Due to the structural obstacles in the ECM and interactions between the ECM constituents and macromolecules, a single, free diffusion coefficient may not be sufficient for characterizing diffusion. In the present work, three different theoretical fitting models were therefore applied and compared.

2 Materials and Methods

2.1 *Fluorescence Correlation Spectroscopy*

FCS is based on recording of intensity fluctuations from fluorescent molecules in the detection volume. Data processing yields a correlation function that compares the signal at time t with the signal at a short time τ later. The normalized autocorrelation function is given by[12]

$$G(\tau) = 1 + \frac{\langle \partial F(t) \cdot \partial F(t+\tau) \rangle}{\langle F(t) \rangle^2} = \frac{\langle F(t) \cdot F(t+\tau) \rangle}{\langle F(t) \rangle^2}, \quad (1)$$

where $F(t)$ is the measured fluorescence signal intensity at time t, and $\partial F(t)$ is the deviation from the mean signal intensity $\langle F(t) \rangle$.

To retrieve relevant information, the correlation function is represented by a proper mathematical model. A general fitting model for multiple diffusive species undergoing free translational diffusion in a 3-D Gaussian detection volume, including a triplet fraction, can be described by[12]

$$G(\tau) = 1 + \frac{1}{\langle N \rangle} \cdot \frac{1 - T + T \exp\left(-\frac{\tau}{\tau_T}\right)}{1 - T} \cdot \left\{ \sum_{i=1}^{m} \frac{\Phi_i}{\left[1 + \left(\frac{\tau}{\tau_{D_i}}\right)\right]\left[1 + \frac{1}{S^2}\left(\frac{\tau}{\tau_{D_i}}\right)\right]^{1/2}} \right\}, \quad (2)$$

where $\langle N \rangle$ is the mean number of particles in the detection volume, T and τ_T are the triplet fraction and triplet lifetime, respectively (both assumed equal for all components), Φ_i is the fractional intensity of the i'th species, m is the total number of species in the sample, and τ_{D_i} is the translational diffusion time of the i'th species through the detection volume.

The structure parameter,

$$S = \omega_z / \omega_{xy}, \quad (3)$$

denotes the ratio of the axial to the radial waist of the Gaussian detection volume, defined as the distances at which the intensity drops to $1/e^2$ of the maximum intensity.[12]

The diffusion coefficient D is calculated by

$$D = \frac{\omega_{xy}^2}{4\tau_D}. \quad (4)$$

For anomalous diffusion, D is the apparent diffusion coefficient and depends on the time scale, or equivalently the length scale, of the experiment.[21] The autocorrelation function for anomalous diffusion can be described by[12]

$$G(\tau) = 1 + \frac{1}{\langle N \rangle} \cdot \frac{1 - T + T \exp\left(-\frac{\tau}{\tau_T}\right)}{1 - T} \cdot \frac{1}{\left[1 + \left(\frac{\tau}{\tau_D}\right)^{\alpha}\right]\left[1 + \frac{1}{S^2}\left(\frac{\tau}{\tau_D}\right)^{\alpha}\right]^{1/2}}, \quad (5)$$

where α is the anomaly coefficient. The value of α indicates the degree of anomaly, and equals 1 for free, Brownian diffusion. Obstructed diffusion is indicated by $\alpha < 1$, and is called anomalous subdiffusion.[7,21,22]

2.2 *Materials and Sample Preparation*

Tetramethylrhodamine (TMR)-dextran, MW 155 kDa (Sigma-Aldrich, Saint Louis, Missouri) and 2 MDa (Molecular Probes, Eugene, Oregon), and 150-kDa Alexa Fluor 546-IgG (Molecular Probes, Eugene, Oregon) were used as fluorescent tracers. TMR and Alexa dyes are highly suitable for FCS due to high quantum yields, photostability, and aqueous solubility.

For maximum detection efficiency, concentrations of the tracers were chosen individually for the different model systems, using a lower limit of photon count rate equal to ten times the background signal[8] of an unstained sample. Due to difficulties dissolving the 2-MDa TMR-dextran molecule, the solution was successively vortexed and heated to 37 °C before filtering through a 0.45-μm membrane filter (Millex-HV, PVDF, Millipore, Billerica, Massachusetts) to eliminate large aggregates. For measurements of free diffusion in solution, the tracers were diluted in phosphate buffered saline (PBS) to concentrations on the order of 10^{-8} M.

Bovine gelatin powder (Kebo, Oslo, Norway) was weighed and dissolved in PBS to produce a hydrogel concentration of 5% (w/v). Tracers were added to final concentrations on the order of 10^{-8} M, and the mixture was given a quick stir before incubation at 45 °C for at least 20 min.

Multicellular spheroids were made from the human osteosarcoma cell line (OHS).[23] Tumor cell populations of 2×10^6 were seeded in 75-cm^2 cell culture flasks (Corning

Incorporated, Corning, New York) precoated with 9 ml of 1% soft agar, and containing 25-ml growth medium (RPMI-1640) supplemented with 10% fetal bovine serum, 100-units/ml penicillin/streptomycin, and 1-mM L-glutamine (all from Sigma-Aldrich, Saint Louis, Missouri). The spheroids were grown at 37 °C and 5% CO_2. Half the growth medium was changed after 3 days, and the spheroids were allowed to grow for 2 more days to reach a convenient size of 150 to 250 μm diameter.[24]

Spheroids were transferred to tubes and tracers were added to final concentrations of 10^{-7} to 10^{-6} M for 155-kDa dextran and 10^{-8} to 10^{-7} M for IgG and 2-MDa dextran. Several concentrations were prepared before each experiment, and the concentration that gave the best signal-to-noise ratio was chosen. FCS measurements were performed after incubation of the spheroids on a roller at 37 °C. The incubation time was 5 to 7 h for the smallest tracers. To ensure penetration into the spheroids, the 2-MDa dextran was allowed 10 to 12 h of incubation.

2.3 *Experimental Setup and Optimization of Parameters*

One-photon FCS measurements were performed using the LSM510/ConfoCor2 (Carl Zeiss Jena GmbH, Germany) with a C-Apochromat 40×/1.2-W corr objective. All tracers were excited by a 543-nm laser, and fluorescence was detected through a BP 560 to 615 filter and a pinhole diameter of 80 μm (1 Airy unit).

The dimension of the detection volume for the 543 HeNe laser line was estimated using rhodamine 6 G (Sigma-Aldrich, Saint Louis, Missouri) with a known diffusion coefficient of $2.8 \cdot 10^{-6}$ cm^2/s. The radial waist was calculated to 0.19 μm using Eq. (4).

Laser powers were kept low (0.9 to 2.3 μW incident on the sample) to avoid artifacts like photobleaching and optical saturation. Photobleaching was indicated by falling baselines in the intensity fluctuation data. Saturation was investigated for all tracers in solution, and was detected as a deviation from linearity between the photon count rate per molecule and laser power. Measured characteristic diffusion times remained constant in the chosen laser power range (data not shown).

To minimize the probability of having to discard data due to tracer aggregates passing through the detection volume, short measurement times were used (2 to 5 s). Statistics were improved by calculating the diffusion coefficients from the average correlation function of several (5 to 30) repetitive runs.[25]

The spheroids were imaged by confocal laser scanning microscopy (CLSM) to define the position of the FCS measurements in the ECM. Cells were visualized by detecting reflection of the argon 488 laser through a BP 480 to 520 filter [Fig. 1(a)], and the labeled macromolecules, which were located in the ECM, were imaged using a HeNe 543 laser and a LP 560 filter [Fig. 1(b)]. The resulting images were sufficient for localizing the extracellular space. The pixel size of the images was 0.11 (zoom 4) to 0.45 μm (zoom 1), i.e., the same order as the radial dimension of the detection volume. FCS measurements were typically performed in extracellular areas with a distance of 4 to 8 μm between cells [Fig. 1(d)]. The extracellular composition has previously been characterized.[26]

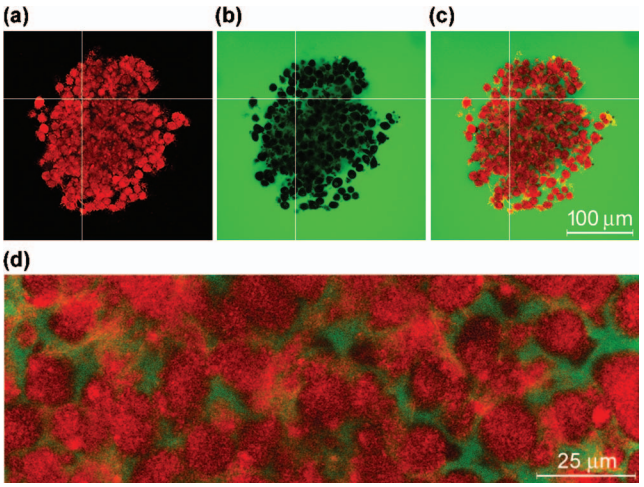

Fig. 1 CLSM image of an OHS multicellular spheroid incubated with Alexa Fluor 546 IgG. (a) Reflection of Ar 488 laser (red), (b) emission (BP 560 to 615 nm) of Alexa Fluor 546 (green), and (c) superposition of both images. The crosshair indicates the localization of the focal volume. (d) An enlarged section of the spheroid indicates the dimensions of the extracellular space.

The measurements were taken at a depth in the spheroids of 20 to 30 μm. FCS could not be performed farther into the spheroids due to scattering and absorption of light, resulting in a low signal-to-noise ratio. Images were compared before and after FCS measurements to exclude measurements influenced by movement artifacts.

2.4 *Data Analysis*

For the 2-MDa TMR-dextran, large peaks in the intensity time traces due to aggregates were carefully deleted from the raw data files. For all tracers, measurements were discarded if the fluctuation data showed a successively falling baseline, or if the normalized autocorrelation curve was distorted in any way. For data analysis, an anomalous fitting model and a two-component free diffusion model were applied whenever the one-component free diffusion model gave an unsatisfactory fit. The available fitting models in the LSM510/ConfoCor2 software are based on Eq. (2) and were used for one- and two-component fittings. The anomalous model based on Eq. (5) was applied using MATLAB (Mathworks Incorporated, Natick, Massachusetts) (gfit; open-source software for global analysis of experimental data, see http://gfit.sourceforge.net/).

A two-sample, two-tailed student's T-test (Minitab, Minitab Incorporated, State College, Pennsylvania) assuming nonequal variances was used to perform statistical comparison of the Gaussian-distributed diffusion coefficients obtained with FCS and FRAP. The Mann-Whitney test was applied when the normality assumption was violated and the sample size was less than 30. A significance criterion of $p \leqslant 0.05$ was used. The goodness of fit was quantified by R^2 (the correlation index).[27] To statistically compare the fitting models, the difference between R^2 for the two-component and the anomalous model ($R^2_{\text{two-component}} - R^2_{\text{anomalous}}$) was calculated for each dataset and grouped according to tracers and model systems. The probability of this difference being equal to zero was tested with a 95% confidence interval.

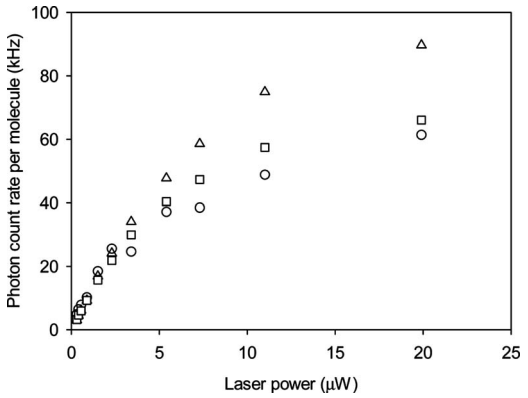

Fig. 2 Investigation of optical saturation for Alexa Fluor 546-IgG (□), 155-kDa TMR-dextran (△), and 2-MDa TMR-dextran (○) in solution. The plot shows the photon count rate per molecule as a function of the laser power incident on the sample.

3 Results

3.1 *Optimization and Calibration of Experimental Setup*

Optimal illumination of the samples was achieved by keeping the laser power at a low level to minimize photobleaching and optical saturation. Photobleaching was occasionally observed as a falling baseline in the fluorescence intensity time traces (data not shown). For all tracers in solution, saturation effects were observed as a deviation from the linear dependence between the photon count rate per molecule and laser power, and occurred above laser powers of 3.4 μW incident on the sample (Fig. 2). Based on this, the maximum laser power used in the FSC experiments was 2.3 μW incident on the sample.

To confirm that our instrumental setup was well calibrated, the diffusion of all tracers was measured in aqueous solution as a first step. As expected, the one-component free diffusion model was found to be appropriate (Table 1). Fitting the anomalous model to measurements of free diffusion in solution yielded average anomaly coefficients for the three tracers in the range of $0.91 < \alpha < 0.93$. Fitting a two-component model to the same experimental data did not give interpretable results, as one of the components indicated unlikely fast diffusion.

3.2 *Diffusion Measurements*

Representative intensity time traces for IgG and dextrans in gel and spheroids are shown in Fig. 3. Aggregates are visible as peaks in the fluctuation data for the 2-MDa dextran. The higher average photon count rate for measurements in sphe-

Table 1 Mean values of experimental diffusion coefficients (10^{-8} cm^2/s) and standard deviations obtained with FCS for IgG and dextrans (155 kDa and 2 MDa) in solution, 5% gelatin hydrogel, and OHS multicellular spheroids. For measurements in solution, the one-component free diffusion model was used. For measurements in gel and spheroids, diffusion coefficients are estimated by the two-component free diffusion model and the anomalous diffusion model. The anomaly coefficients α are presented, together with the anomalous diffusion coefficients.

System	One-component free or anomalous diffusion		Two-component free diffusion	
	D	α	*D*1	*D*2
150-kDa IgG				
Solution	31.99±0.88	-	-	-
Gel	9.65±3.01	0.76±0.04	14.42±3.93	1.58±1.08
Spheroids	20.95±4.83	0.81±0.05	22.51±4.49	1.96±1.41
155-kDa dextran				
Solution	18.13±1.64	-	-	-
Gel	5.81±1.13	0.82±0.08	16.26±8.86	2.97±1.52
Spheroids	12.68±2.79	0.86±0.09	17.28±3.65	2.77±2.07
2-MDa dextran				
Solution	7.33±0.95	-	-	-
Gel	2.97±0.42	0.85±0.06	12.86±6.06	1.35±0.56
Spheroids	1.23±0.32	0.81±0.08	4.81±2.62	0.54±0.31

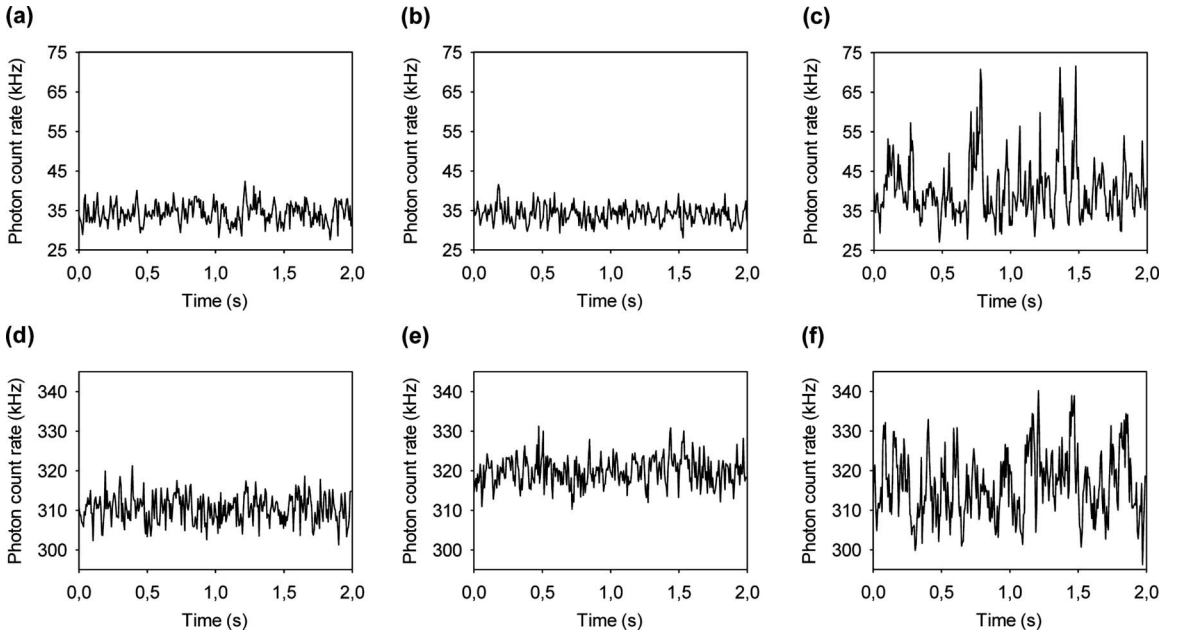

Fig. 3 Intensity fluctuations during the measurement for (a) and (d) Alexa Fluor 546–IgG, (b) and (e) 155-kDa TMR-dextran, and (c) and (f) 2-MDa TMR-dextran in (a), (b), and (c) 5% gelatin hydrogel, and (d), (e), and (f) OHS multicellular spheroids.

roids reflects the higher concentration of tracer needed to overcome the cellular autofluorescence. Typically, the one-component free diffusion model failed when fitted to the autocorrelation curves obtained from measurements in gel and spheroids. An anomalous diffusion model and a free diffusion model with two species were therefore applied (Table 1), as shown for IgG in Fig. 4. However, the quality of fit by the two latter models could not be distinguished based on R^2.

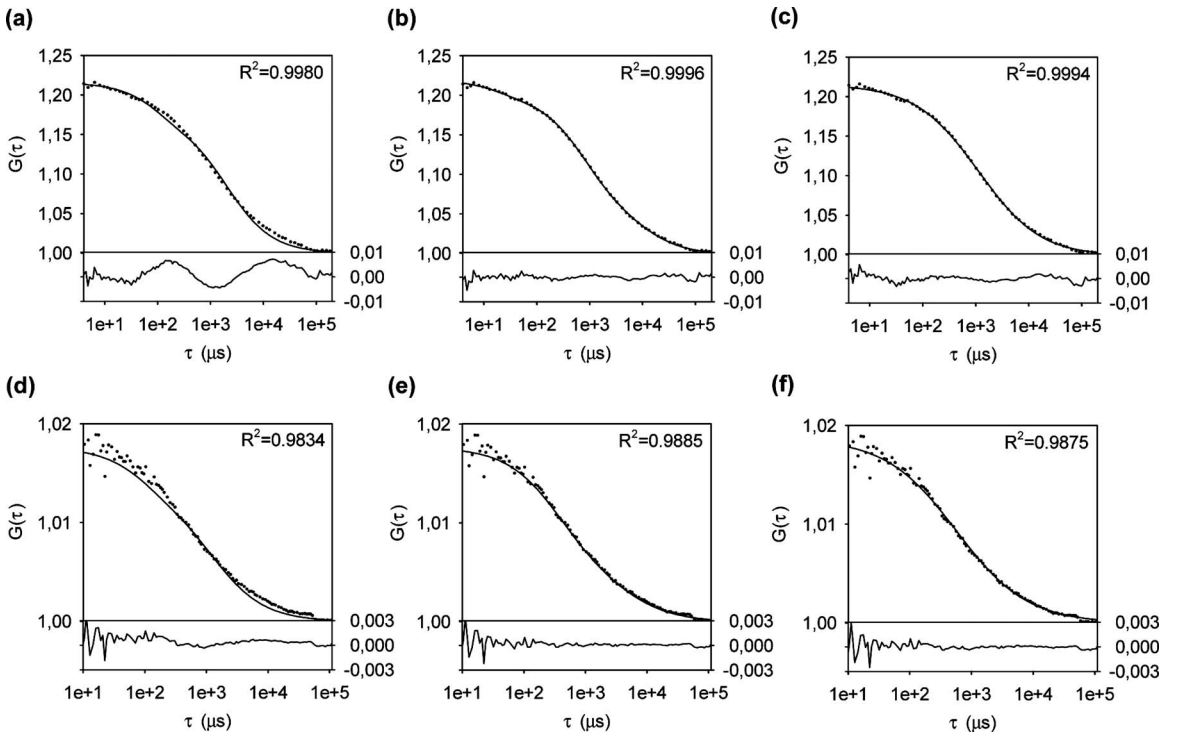

Fig. 4 Autocorrelation function (…….) and curve fitting (—) by (a) and (d) one-component, (b) and (e) anomalous, and (c) and (f) two-component model for (a), (b), and (c) IgG in 5% gelatin hydrogel and (d), (e), and (f) OHS multicellular spheroids. The goodness of fit is indicated by R^2, and residuals are shown in the lower part of each panel.

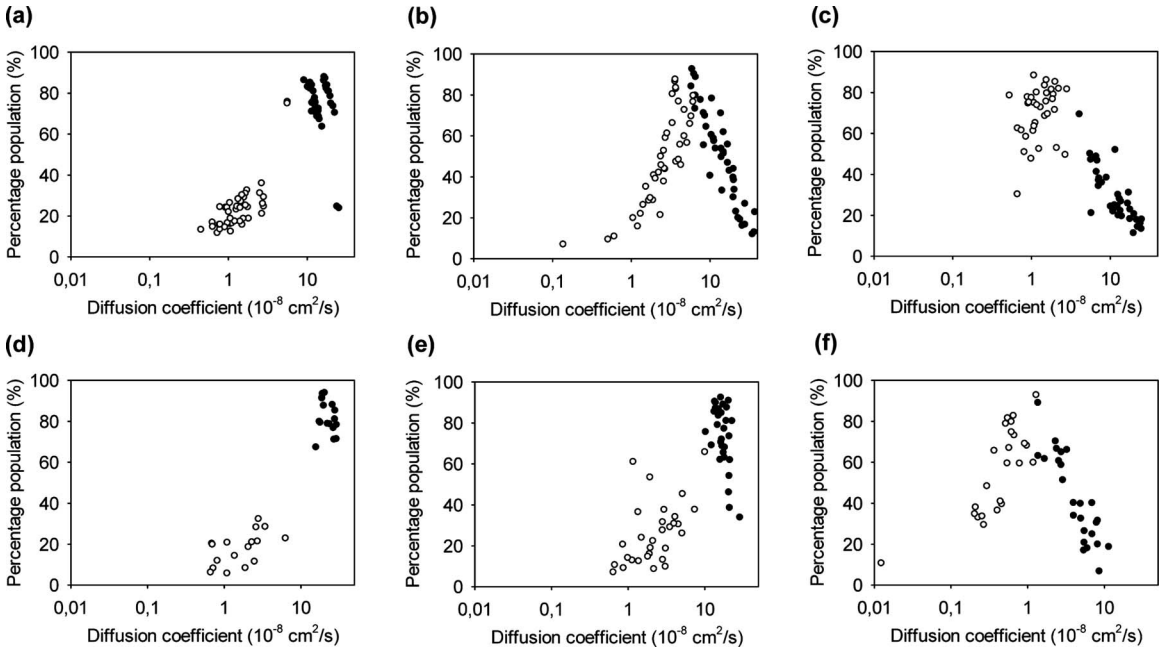

Fig. 5 Percentage populations of the fast (●) and slow (○) diffusion components obtained by fitting the two-component free diffusion model for (a) and (d) IgG, (b) and (e) 155-kDa dextran, and (c) and (f) 2-MDa dextran in (a), (b), and (c) 5% gelatin hydrogel and (d), (e), and (f) OHS multicellular spheroids.

Using the anomalous model, all three tracers showed subdiffusive properties in both gel and spheroids. The two-component model gave significantly different diffusion coefficients for the two components. The ratios of the fast to slow diffusing components were in the range of 5 to 11. The average populations (Fig. 5) of the two diffusing components were especially well separated for IgG. For IgG in gel, a further separation in two groups can be seen within each component [Fig. 5(a)]. This reflects the variability between gels produced on two different days. In gel, the ratios of the diffusion coefficients of the fast components relative to those in solution were 0.45, 0.90, and 1.75, and the percentage populations of the fast components were (75 ± 13), (50 ± 23), and $(30 \pm 13)\%$ for IgG, 155-kDa dextran, and 2-MDa dextran, respectively. In spheroids, the ratios of the diffusion coefficients of the fast components relative to those in solution were 0.71, 0.95, and 0.66, and the percentage populations of the fast components were (82 ± 8.1), (74 ± 16), and $(42 \pm 22)\%$ for IgG, 155-kDa dextran, and 2-MDa dextran, respectively.

Diffusion coefficients obtained from the one-component free diffusion model for solution and the anomalous model for gel and spheroids were compared (Fig. 6). The diffusion coefficients in solution, gel, and spheroids are significantly different for all tracers. The diffusion coefficients for 2-MDa dextran are significantly lower than for the smaller molecules in all model systems. IgG experienced a significantly faster diffusion than 155-kDa dextran in all model systems. The ratios of the diffusion coefficients in gel to those in solution are approximately the same (0.30 to 0.41) for all tracers. Diffusion measured extracellularly in spheroids is approximately twice as fast as in gels for both IgG and 155-kD dextran. The 2-MDa molecule, on the other hand, experiences a markedly retarded diffusion in spheroids. The ratios of the diffusion coefficients in spheroids to those in solution are approximately 0.66 and 0.70 for IgG and 155-kDa dextran, respectively, and 0.16 for 2-MDa dextran.

3.3 *Comparison of Diffusion Coefficients Measured with Fluorescence Correlation Spectroscopy and Fluorescence Recovery after Photobleaching*

Anomalous diffusion coefficients determined by FCS was compared to free diffusion coefficients obtained with FRAP[17] for tracers in solution, 5% gelatin hydrogel, and OHS multicellular spheroids (Fig. 7). The FRAP measurements, which were previously performed in our laboratory, were best repre-

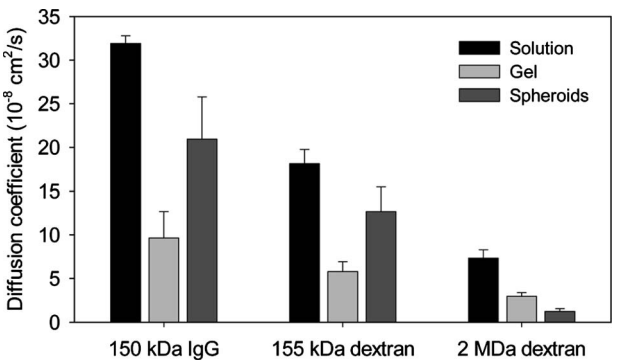

Fig. 6 Mean diffusion coefficients with standard deviations for IgG, 155-kDa dextran, and 2-MDa dextran in solution (black), 5% gelatin hydrogel (light gray), and OHS multicellular spheroids (dark gray). Diffusion coefficients for measurements in solution are based on the one-component free diffusion model, whereas the anomalous diffusion model was used to estimate diffusion coefficients in gel and spheroids. Mean values represent 18 to 45 measurements.

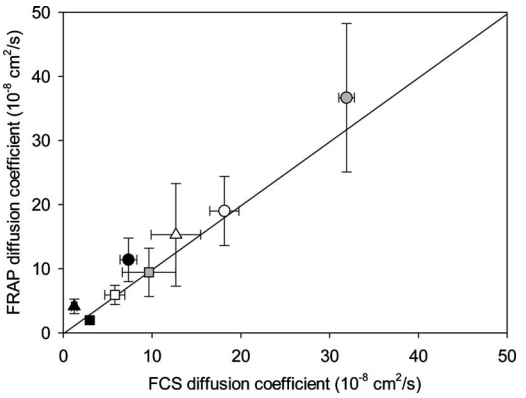

Fig. 7 Mean diffusion coefficients calculated from FCS and FRAP measurements of IgG (gray), 155-kDa dextran (white), and 2-MDa dextran (black) in solution (circle), 5% gelatin hydrogel (square), and OHS multicellular spheroids (triangle). Standard deviations are indicated by error bars. The one-component free diffusion model was used for FRAP in all model systems and for FCS in solution, whereas the anomalous diffusion model was applied for FCS in gel and spheroids. Mean FCS values represent 18 to 45 measurements. FRAP measurement of FITC-IgG in spheroids was not obtained due to internalization of the labeled molecules into the cells.

sented by the one-component free diffusion model. The differences between the diffusion coefficients estimated by the two techniques are in the range of one standard deviation.

4 Discussion

One-photon FCS measurements of macromolecular diffusion in solution, 5% gelatin hydrogel, and extracellularly in OHS multicellular spheroids were successfully achieved and compared to previously reported two-photon FRAP data.[17] A novel aspect is to use FCS to measure extracellular diffusion in multicellular spheroids, which is a well-established model for avascular tumor tissue.[4,24,28,29] Whereas FRAP has been used for this purpose,[4,30] no FCS studies on extracellular diffusion in multicellular spheroids have, to our knowledge, previously been published. In the present study, the main goal was to investigate whether FCS measurements give comparable results to FRAP data obtained on the same microscope, and whether results obtained with FCS indicate anomalous or multiphase diffusion, and thereby provide additional information to FRAP.

4.1 *Diffusion of Macromolecules in 5% Gelatin Hydrogel Multicellular Spheroids*

The diffusion coefficient for dextrans decreased with increasing molecular size. IgG experienced a faster diffusion than the dextran of approximately the same size. This has been previously reported,[31] and is due to the configurational difference between the globular IgG and the linear, flexible dextran.

The diffusion of IgG and dextrans in gel and spheroids was slower than in solution, and deviated from the one-component free diffusion model. This demonstrates that molecular mobility is subject to obstruction by the polymer network. However, tracer aggregates or a distorted Gaussian focus profile may also cause the one-component free diffusion model to fail, giving an erroneous impression of anomalous or multiphase diffusion.[19] To avoid distortion of the focus profile, the laser power was kept low.

Fitting of the anomalous model to autocorrelation functions for all three tracers in gel and spheroids yielded anomaly coefficients close to, but significantly different from, the anomaly coefficients measured in solution. This result is supported by a diffusion study conducted by Lead, Starchev, and Wilkinson,[32] which showed that increasing a gel concentration from 0 to 3% resulted in only a slight increase of anomaly. Anomalous diffusion in heterogeneous systems has been reported in several FCS studies.[7,9,11,21,32–34] Various underlying causes for anomalous diffusion have been suggested, such as molecular binding of the diffusing particles,[35] adsorption to chains in the structural meshwork,[34] molecular crowding,[11] and infrequent and large jumps that particles make between distinct pores in the network in which they are constrained.[36]

The two-component diffusion model was successfully fitted to all measurements in gel and spheroids. In all cases, the diffusion coefficients of the two components were significantly different. The fastest diffusion components were found to be of the same order as the free diffusion coefficient measured in solution, hence indicating an aqueous phase. Only for the 2-MDa dextran in gel was the fast component significantly higher than the free diffusion coefficient in solution. The slow components were five to eleven times slower than the fast components.

It has been suggested that the interstitial space consists of two phases; a viscous gel compartment and a free-fluid space, which offers less resistance to interstitial transport,[37,38] thus supporting the relevance of the two-component model. FCS has also revealed a two-phase diffusion process in tumors.[10] However, in complex and heterogeneous environments like the interstitium, molecules may aggregate, bind to structures of various sizes, or be trapped in compartments. Diffusion may thus be more diverse than what can be represented by the two-component model.

To determine whether diffusion is anomalous or if there are, in fact, two components diffusing with different speed, would give valuable information about the structural geometry of the ECM and interactions between the ECM and the diffusing particles. However, based on visual inspection of the curve fits and the corresponding residuals, together with a statistical analysis of R^2, it was not possible to conclude which model gives a true representation of the diffusion process. This is in accordance with previous findings of molecular dynamics in complex systems.[7,9,33] On the other hand, several factors suggest that the two-component model is less reliable, the lack of a visible two-component shape of the autocorrelation curve, the unlikely high diffusion coefficient of the fast component for 2-MDa dextran in gel, and the large standard deviations for the mean diffusion coefficients calculated from the two-component model (Table 1). The fact that the anomalous model fits the data equally well with a lower number of variables further suggests that this model is more robust.

4.2 *Relevance of Tissue Models*

Gelatin hydrogel mimics the structural collagen network in the ECM, and the multicellular spheroid represents a 3-D *in-*

vitro model of an avascular tumor.[28] A gelatin gel of 5% has a density of collagen fibers comparable to the collagen content in the ECM of tissue, which is reported to be 0.2 to 2%.[39,40] The collagen concentration in OHS multicellular spheroids, however, has been measured to 0.05% (unpublished data). Also other multicellular spheroids have been shown to have ten times less collagen content compared to the corresponding xenografts growing *in vivo*.[4] In the present study, diffusion is clearly more obstructed in gel than in spheroids for IgG and 155-kDa dextran. However, in contrast to the two smaller molecules, the 2-MDa dextran experiences a slower diffusion in the ECM than in gel. This indicates that up to a certain size, the particles are mainly retarded because of their molecular shape and increased viscosity of the solvent. For the 2-MDa molecule, however, the size of the particle relative to the mesh size of the geometrical network provides an additional retarding factor. The ECM is therefore a more severe barrier for larger molecules.

4.3 *Fluorescence Correlation Spectroscopy Compared to Fluorescence Recovery after Photobleaching*

One-photon FCS data were compared to results previously obtained with two-photon FRAP.[17] The FCS measurements revealed both anomalous and two-component diffusion, which were not detectable in the FRAP study. This demonstrates that FCS is a more sensitive technique than FRAP, and provides information with a higher time resolution. The anomaly coefficients for the FCS data indicate little deviation from free diffusion, and we therefore assume that the anomalous diffusion coefficients can be compared to the free diffusion coefficients obtained with FRAP. Except for the 2-MDa molecule, diffusion coefficients from FCS measurements equal the FRAP diffusion coefficients within the range of one standard deviation. This demonstrates that although the two methods differ in principle and in practical applications, FCS and FRAP can be applied to the same system within a certain time scale of the molecular dynamics.

FCS and FRAP are both based on fluorescence detection, and are commonly used in diffusion studies.[4,10,11,18,33,39] There are, however, several fundamental differences between the two methods, making them suitable for different purposes. FRAP is based on equilibrium perturbation by photobleaching of a predefined area with a high laser intensity and subsequently detecting the influx of unbleached tracers. The photobleaching process may induce uncharacterized chemical and biological disturbances in the sample. In FCS, the system is in equilibrium throughout the FCS measurement, and photobleaching is avoided by using low laser intensities. This implies that the two techniques require fluorophores with different photostability. In addition, whereas one single particle is detectable in FCS, high concentrations are required to perform a FRAP experiment. FCS is thus less invasive than FRAP when studying living tissue, because substantially less chemical substance is injected and no perturbation of the system occurs. For measuring immobile fractions, FRAP is a better suited technique because FCS cannot detect immobile or very slowly moving particles. For small particles in solution, the diffusion is too rapid for FRAP detection, but ideal for FCS. Another advantage of FCS over FRAP is that it is a more versatile technique, giving information about translational and rotational diffusion, triplet fractions, interactions, and concentrations.

5 Conclusion

The present work demonstrates that one-photon FCS is suitable for measuring diffusion of macromolecules extracellularly in tissue. One-photon FCS and two-photon FRAP[17] measurements on the LSM510/ConfoCor2 gave comparable diffusion coefficients. In addition, FCS revealed a two-phase or an anomalous nature of the transport in gel and spheroids, which was not possible to detect with FRAP performed on the same microscope.

FCS is an important technique for studying the delivery of macromolecules in cancer therapy. The method may provide information about the interactions and transport barriers extracelluarly as well as intracellularly.[18] FCS and related techniques[41–44] are constantly being refined, and are valuable tools for investigating fundamental processes in molecular biology.

Acknowledgments

We gratefully acknowledge Mikhail Levin, UCHC, Farmington, Connecticut, for assistance on the *gfit* software; Kristin Sæterbø, Department of Physics, NTNU, for cultivating cells; and Henning Omre, Department of Mathematical Sciences, NTNU, for advice on statistical analysis. The work was supported by the Norwegian Cancer Society.

References

1. L. Eikenes, Ø. S. Bruland, C. Brekken, and C. de L. Davies, "Collagenase increases the transcapillary pressure gradient and improves the uptake and distribution of monoclonal antibodies in human osteosarcoma xenografts," *Cancer Res.* **64**(14), 4768–4773 (2004).
2. M. Ferrari, "Cancer nanotechnology: Opportunities and challenges," *Nat. Rev. Cancer* **5**(3), 161–171 (2005).
3. Y. Boucher, L. T. Baxter, and R. K. Jain, "Interstitial pressure-gradients in tissue-isolated and subcutaneous tumors-implications for therapy," *Cancer Res.* **50**(15), 4478–4484 (1990).
4. C. de L. Davies, D. A. Berk, A. Pluen, and R. K. Jain, "Comparison of IgG diffusion and extracellular matrix composition in rhabdomyosarcomas grown in mice versus *in vitro* as spheroids reveals the role of host stromal cells," *Br. J. Cancer* **86**(10), 1639–1644 (2002).
5. D. Magde, E. Elson, and W. W. Webb, "Thermodynamic fluctuations in a reacting system-measurement by fluorescence correlation spectroscopy," *Phys. Rev. Lett.* **29**(11), 705–708 (1972).
6. R. Rigler, Ü. Mets, J. Widengren, and P. Kask, "Fluorescence correlation spectroscopy with high count rate and low background: analysis of translational diffusion," *Eur. Biophys. J.* **22**(3), 169–175 (1993).
7. M. Wachsmuth, W. Waldeck, and J. Langowski, "Anomalous diffusion of fluorescent probes inside living cell nuclei investigated by spatially-resolved fluorescence correlation spectroscopy," *J. Mol. Biol.* **298**(4), 677–689 (2000).
8. P. Schwille, U. Haupts, S. Maiti, and W. W. Webb, "Molecular dynamics in living cells observed by fluorescence correlation spectroscopy with one- and two-photon excitation," *Biophys. J.* **77**(4), 2251–2265 (1999).
9. M. Weiss, H. Hashimoto, and T. Nilsson, "Anomalous protein diffusion in living cells as seen by fluorescence correlation spectroscopy," *Biophys. J.* **84**(6), 4043–4052 (2003).
10. G. Alexandrakis, E. B. Brown, R. T. Tong, T. D. McKee, R. B. Campbell, Y. Boucher, and R. K. Jain, "Two-photon fluorescence correlation microscopy reveals the two-phase nature of transport in tumors," *Nat. Med.* **10**(2), 203–207 (2004).
11. M. Weiss, M. Elsner, F. Kartberg, and T. Nilsson, "Anomalous subdiffusion is a measure for cytoplasmic crowding in living cells," *Biophys. J.* **87**(5), 3518–3524 (2004).

12. K. Weisshart, V. Jüngel, and S. J. Briddon, "The LSM 510 META-ConfoCor 2 system: an integrated imaging and spectroscopic platform for single-molecule detection," *Curr. Pharm. Biotechnol.* **5**(2), 135–154 (2004).
13. I. Gregor, D. Patra, and J. Enderlein, "Optical saturation in fluorescence correlation spectroscopy under continuous-wave and pulsed excitation," *ChemPhysChem* **6**(1), 164–170 (2005).
14. G. Nishimura and M. Kinjo, "Systematic error in fluorescence correlation measurements identified by a simple saturation model of fluorescence," *Anal. Chem.* **76**(7), 1963–1970 (2004).
15. D. Axelrod, D. E. Koppel, J. Schlessinger, E. Elson, and W. W. Webb, "Mobility measurement by analysis of fluorescence photobleaching recovery kinetics," *Biophys. J.* **16**(9), 1055–1069 (1976).
16. T. K. L. Meyvis, S. C. De Smedt, P. Van Oostveldt, and J. Demeester, "Fluorescence recovery after photobleaching: a versatile tool for mobility and interaction measurements in pharmaceutical research," *Pharm. Res.* **16**(8), 1153–1162 (1999).
17. E. A. Schnell, L. Eikenes, I. Tufto, A. Erikson, A. Juthajan, M. Lindgren, and C. de L. Davies, "Diffusion measured by fluorescence recovery after photobleaching based on multiphoton excitation laser scanning microscopy," submitted to *J. Biomed. Opt.* (2008).
18. J. P. Clamme, G. Krishnamoorthy, and Y. Mély, "Intracellular dynamics of the gene delivery vehicle polyethylenimine during transfection: investigation by two-photon fluorescence correlation spectroscopy," *Biochim. Biophys. Acta* **1617**(1–2), 52–61 (2003).
19. S. T. Hess and W. W. Webb, "Focal volume optics and experimental artifacts in confocal fluorescence correlation spectroscopy," *Biophys. J.* **83**(4), 2300–2317 (2002).
20. S. A. Tatarkova, A. K. Verma, D. A. Berk, and C. J. Lloyd, "Quantitative fluorescence microscopy of macromolecules in gel and biological tissue," *Phys. Med. Biol.* **50**(23), 5759–5768 (2005).
21. D. S. Banks and C. Fradin, "Anomalous diffusion of proteins due to molecular crowding," *Biophys. J.* **89**(5), 2960–2971 (2005).
22. A. Masuda, K. Ushida, and T. Okamoto, "New fluorescence correlation spectroscopy enabling direct observation of spatiotemporal dependence of diffusion constants as an evidence of anomalous transport in extracellular matrices," *Biophys. J.* **88**(5), 3584–3591 (2005).
23. Ø. Fodstad, A. Brøgger, Ø. Bruland, Ø. P. Solheim, J. M. Nesland, and A. Pihl, "Characteristics of a cell-line established from a patient with multiple osteosarcoma, appearing 13 years after treatment for bilateral retinoblastoma," *Int. J. Cancer* **38**(1), 33–40 (1986).
24. M. H. Hjelstuen, K. Rasch-Halvorsen, C. Brekken, Ø. Bruland, and C. de L. Davies, "Penetration and binding of monoclonal antibody in human osteosarcoma multicell spheroids: Comparison of confocal laser scanning microscopy and autoradiography," *Acta Oncol.* **35**(3), 273–279 (1996).
25. O. Krichevsky and G. Bonnet, "Fluorescence correlation spectroscopy: the technique and its applications," *Rep. Prog. Phys.* **65**(2), 251–297 (2002).
26. C. de L. Davies, H. Müller, I. Hagen, M. Gårseth, and M. H. Hjelstuen, "Comparison of extracellular matrix in human osteosarcomas and melanomas growing as xenografts, multicellular spheroids, and monolayer cultures," *Anticancer Res.* **17**(6D), 4317–4326 (1997).
27. A. M. Brown, "A step-by-step guide to non-linear regression analysis of experimental data using a Microsoft Excel spreadsheet," *Comput. Methods Programs Biomed.* **65**, 191–200 (2001).
28. R. M. Sutherland, "Cell and environment interactions in tumor microregions-the multicell spheroid model," *Science* **240**(4849), 177–184 (1988).
29. M. H. Hjelstuen, K. Rasch-Halvorsen, Ø. Bruland, and C. de L. Davies, "Uptake, penetration, and binding of monoclonal antibodies with increasing affinity in human osteosarcoma multicell spheroids," *Anticancer Res.* **18**(5A), 3153–3161 (1998).
30. H. Sauer, V. Pütz, K. Fischer, J. Hescheler, and M. Wartenberg, "Increased doxorubicin uptake and toxicity in multicellular tumour spheroids treated with DC electrical fields," *Br. J. Cancer* **80**(8), 1204–1213 (1999).
31. D. A. Berk, F. Yuan, M. Leunig, and R. K. Jain, "Fluorescence photobleaching with spatial Fourier-analysis: measurement of diffusion in light-scattering media," *Biophys. J.* **65**(6), 2428–2436 (1993).
32. J. R. Lead, K. Starchev, and K. J. Wilkinson, "Diffusion coefficients of humic substances in agarose gel and in water," *Environ. Sci. Technol.* **37**(3), 482–487 (2003).
33. P. Schwille, J. Korlach, and W. W. Webb, "Fluorescence correlation spectroscopy with single-molecule sensitivity on cell and model membranes," *Cytometry* **36**(3), 176–182 (1999).
34. G. C. Fadda, D. Lairez, B. Arrio, J. P. Carton, and V. Larreta-Garde, "Enzyme-catalyzed gel proteolysis: an anomalous diffusion-controlled mechanism," *Biophys. J.* **85**(5), 2808–2817 (2003).
35. M. J. Saxton, "Anomalous diffusion due to binding: a Monte Carlo study," *Biophys. J.* **70**(3), 1250–1262 (1996).
36. I. Y. Wong, M. L. Gardel, D. R. Reichman, E. R. Weeks, M. T. Valentine, A. R. Bausch, and D. A. Weitz, "Anomalous diffusion probes microstructure dynamics of entangled F-actin networks," *Phys. Rev. Lett.* **92**(17), 178101 (2004).
37. R. K. Jain, "Transport of molecules in the tumor interstitium: a review," *Cancer Res.* **47**(12), 3039–3051 (1987).
38. C. A. Wiederhielm, "Dynamics of capillary fluid exchange: A nonlinear computer simulation," *Microvasc. Res.* **18**, 48–82 (1979).
39. P. A. Netti, D. A. Berk, M. A. Swartz, A. J. Grodzinsky, and R. K. Jain, "Role of extracellular matrix assembly in interstitial transport in solid tumors," *Cancer Res.* **60**(9), 2497–2503 (2000).
40. C. de L. Davies, B. Ø. Engesæter, I. Haug, I. W. Ormberg, J. Halgunset, and C. Brekken, "Uptake of IgG in osteosarcoma correlates inversely with interstitial fluid pressure, but not with interstitial constituents," *Br. J. Cancer* **85**(12), 1968–1977 (2001).
41. N. O. Petersen, "Scanning fluorescence correlation spectroscopy. I. Theory and simulation of aggregation measurements," *Biophys. J.* **49**(4), 809–815 (1986).
42. J. Ries and P. Schwille, "Studying slow membrane dynamics with continuous wave scanning fluorescence correlation spectroscopy," *Biophys. J.* **91**(5), 1915–1924 (2006).
43. M. A. Digman, P. Sengupta, P. W. Wiseman, C. M. Brown, A. R. Horwitz, and E. Gratton, "Fluctuation correlation spectroscopy with a laser-scanning microscope: Exploiting the hidden time structure," *Biophys. J.* **88**(5), L33–L36 (2005).
44. R. P. Kulkarni, D. D. Wu, M. E. Davis, and S. E. Fraser, "Quantitating intracellular transport of polyplexes by spatio-temporal image correlation spectroscopy," *Proc. Natl. Acad. Sci. U.S.A.* **102**(21), 7523–7528 (2005).